Colloids and Surfaces B: Biointerfaces 146 (2016) 180–187

Contents lists available at ScienceDirect

Colloids and Surfaces B: Biointerfaces

journal homepage: www.elsevier.com/locate/colsurfb

The rheological properties of beta amyloid Langmuir monolayers: Comparative studies with melittin peptide

Benjamín Caruso, Ernesto E. Ambroggio, Natalia Wilke, Gerardo Daniel Fidelio*

CIQUIBIC, Departamento de Química Biológica, Facultad de Ciencias Químicas, CONICET, Universidad Nacional de Córdoba, Argentina

ARTICLE INFO

Article history:
Received 29 January 2016
Received in revised form 24 May 2016
Accepted 1 June 2016
Available online 3 June 2016

Keywords:
Elastic shear
Membrane disrupting peptides
Secondary structure
Rheological behavior
Peptide Langmuir monolayers

ABSTRACT

We determined the rheological properties of β-amyloid Langmuir films at the air/water interface, a peptide whose interfacial structure is extended β-sheet, and compared them with those of films composed of Melittin (Mel), which adopts an α-helical conformation at neutral pH. To determine the dilatational and shear moduli we evaluated the response of pure peptide monolayers to an oscillatory anisotropic compressive work. Additionally, a micro-rheological characterization was performed by tracking the diffusion of micrometer sized latex beads onto the interface. This technique allowed us the detection of different rheological behaviour between monolayers presenting a low shear response. Monolayers of the β-sheet structure-adopting peptides, such as β-amyloid peptides, exhibited a marked shear (elastic) modulus even at low surface pressures. In contrast, Mel monolayers exhibited negligible shear modulus and the micro-rheological shear response was markedly lower than that observed for either Aβ1-40 or Aβ1-42 amyloid peptides. When Mel monolayers were formed at the interface of an aqueous solution at pH 11, we observed an increase in both the lateral stability and film viscosity as detected by a slower diffusion of the latex beads, in keeping with an increase in β-sheet structure at this high pH (verified by ATR and FT-IR measurements). We suggest that the interactions responsible for the marked response upon shear observed for β-amyloid peptide monolayers are the hydrogen bonds of the β-sheet structure that can form an infinite planar network at the interface. Conversely, α-helical Mel peptide lack of these inter-molecular interactions and, therefore the shear contribution was negligible. We propose that the secondary structure is important for modulating the rheological behavior of short peptide monolayers regardless of the mass density or surface charge at the surface.

1. Introduction

The rheological study of interfaces covered with proteins is receiving interest from several areas of biology and engineering (including food technology), since proteins have the propensity to adsorb to interfaces and form highly stable films [1,2]. The presence of proteins in such interfaces may impart important stability characteristics to membranes and dispersions, for example, stabilization (and birth) of lipid droplets in the endoplasmic reticulum, lipoproteins, technological emulsions and foams [1,3]. In contrast to most lipid monolayers (except for some long chain ceramides [4]) many peptide monolayers exhibit non-negligible elastic and/or viscous shear moduli that could be quantified by a wide variety of methods [5–7]. Many factors can account for a viscoelastic shear behaviour, associated with a 2D network, such as intermolecular interactions (disulphide bridges, repulsive interactions at close packing or hydrogen bonding) or interdomain interactions [8]. Although several papers have been published on the surface shear behaviour of protein layers, a quantitative relationship of this property to any fundamental parameter like the adsorbed amount [8] or the protein secondary structure is still lacking. In this sense, the work of Cicuta *et al.* [9] provides an approach for assessing the rheological properties of spread protein films describing how the dilatational and shear moduli are related to the surface concentration and to the equilibrium osmotic pressure which allow them to propose that the shear contribution emerges as a consequence of steric jamming (*i.e.*, the dynamical arrest due to surface crowding, where each particle is effectively caged by the neighbouring hard-core repulsive interactions). Most of the data on interfacial rheology of proteins (reviewed in [1–3,10]) deal with adsorbed layers at the

Abbreviations: Mel, Melittin; Aβ1-40 and Aβ1-42, variants 1-40 and 1-42 of the β-amyloid peptides.

* Corresponding author at: CIQUIBIC, Departamento de Química Biológica, Facultad de Ciencias Químicas, Universidad Nacional de Córdoba. Pabellón Argentina, Ciudad Universitaria, X5000HUA Córdoba, Argentina.
E-mail addresses: gerardo.fidelio@gmail.com, gfidelio@fcq.unc.edu.ar (G.D. Fidelio).

http://dx.doi.org/10.1016/j.colsurfb.2016.06.003
0927-7765/

air-water interface. However, in order to describe those factors that may account for each rheological behaviour, spread monolayers appear to be the more appropriate since the surface density and lateral packing can be more accurately tuned than adsorbed films.

Work from our laboratory and others, demonstrated that secondary structure is determinant for peptide monolayer stability and overall compressibility [11,12], the latter being analysed without considering each rheological contribution. Thus, it would be of interest to evaluate if the secondary structure impacts on the surface rheological parameters of peptide films explaining the surface stability and rigidity upon compression. Connected to this, by combining PM-IRRAS and rheological techniques, Renault *et al.* [13] reported that an increase in the shear elastic modulus correlates with the contribution of intermolecular β-sheets in adsorbed ovalbumin monolayers. Thus, the formation of a cohesive interfacial film has been linked with the development of a 2D β-sheet network [13] and, as in the case of β-lactoglobulin, in the way of presentation of fibrils to the water interface [14].

In the present work, we choose to study the rheological features of spread peptide monolayers whose surface properties and interaction with membranes are well characterized, the β-amyloid peptides: Aβ1-40 and Aβ1-42 and Melittin (Mel).

These peptides present a well-defined secondary structure when spread at the air-water interface. The lytic Mel, a 26 residues length peptide, forms stable films at air water interface adopting an α-helix secondary structure at neutral pH subphase [12,15]. This was determined by PM-IRRAS studies of spread Mel monolayers over subphase at pH ~6 [12,16,17]. Conversely, both amyloid peptide Aβ1-40 and Aβ1-42 have almost identical surface behaviour developing highly stable monolayers (Ref. [18] and this paper) with a prevalence of β-sheet structure at an air-water interface [19,20]. These two, rather short kind of peptides (Mel and amyloid peptides), form stable spread monolayers with defined secondary structure, making them adequate model systems to shed light on how secondary structure correlates with interfacial peptide rheology. This work aims to contribute to the elucidation of general features determining the rheological properties of peptide monolayers and its relation to the peptide secondary structure. Furthermore, considering that the selected peptides have been reported to damage membranes [18,21–28] our findings may bring out useful evidence to design experiments directed to study their mechanism of membrane disruption.

2. Material and methods

2.1. Reagents

Melittin (GIGAVLKVLTTGLPALISWIKRKRQ) was purchased from Sigma Chem. Co. (USA) and further purified to be free of phospholipase A_2 as described by Mollay et al. [29]. Aβ1-40 and Aβ1-42 (D^1AEFRHDSGYEVHHQKLVFFAEDVGSNKGAIIGLMVGGVV^{40}**IA**^{42}), were generously gifted by Dr. Frances Separovic (School of Chemistry, Bio21 Institute, The University of Melbourne, Melbourne, Victoria, Australia); NaCl from J.T. Baker was purchased to local distributor. Micrometer-sized beads (0.9 μm diameter, carboxylate-modified beads) were purchased from Sigma Chem. Co. (USA). The water used for the subphase was from a MilliQ system (Millipore, USA) with a resistivity of 18.2 MΩ cm and a surface tension of 72 mN m^{-1}.

2.2. Peptide monolayer formation and compression isotherms

Peptide monolayers were formed using a Langmuir trough containing a 180 mL of unbuffered subphase with 145 mM NaCl, pH 5.6. The final pH of the subphase was set with concentrated NaOH for experiments at higher pH and their value was rechecked after each experiment in order to discard acidification due to atmospheric CO_2. Peptides were dissolved in DMSO to 1 nmol μL^{-1} and, from this solution, they were directly spread onto the aqueous surface. The lateral pressure (determined with a Pt plate using the Wilhelmy method) and the total film area were continuously recorded at a compression rate in between 2 and 5 Å^2 molecule^{-1} min^{-1}. The temperature was maintained at 24.0 ± 0.4 °C using an external Haake bath. Compression isotherms of peptides monolayers were almost identical to those previously published (see Results section). For Brewster Angle Microscopy and oscillation experiments a KSV mini-through (KSV Instruments® Ltd.) was used. For bead diffusion experiments a Microtrough-XS (Kibron®, Finland) was employed.

2.3. Brewster angle microscopy

Monolayers were spread over a Langmuir film balance, as described above, and were directly observed along compression using a Brewster angle microscope coupled to an EP3 Imaging Ellipsometer equipment (Accurion, Goettingen, Germany) with a 20× objective (Nikon, Japan, NA 0.35). For each image acquisition, the monolayer was compressed until reaching the desired lateral pressure, the compression was stopped at this lateral packing, and 3–5 images of different regions of the monolayer were taken. During image acquisition (5–20 s) the lateral pressure did not exhibit any detectable variation.

2.4. Oscillation experiments

These experiments were carried out as previously described [30,31] following the procedures detailed by Cicuta and Terentjev [9]. Briefly, Langmuir peptide film under study was isometrically compressed with two barriers (*i.e.*, anisotropically) up to the desired lateral pressure. Then, sinusoidal area perturbations were performed while measuring both the surface pressure and the phase shift between the tension and the surface area signals. Since the deformation created by the moving barrier is uniaxial, the surface pressure is a superposition of well-defined dilatation and shear. Therefore, taking into account that the interfacial tension is a tensorial quantity, the measured values depend on the direction of the axis along which the stress acts [32]. For this reason, if two Wilhelmy plates are placed in orthogonal positions, the following equations describe the response of the system:

$$|\varepsilon^* + G^*| = A_0 \frac{\Delta\Pi_{\parallel}}{\Delta A} \quad (1)$$

$$|\varepsilon^* - G^*| = A_0 \frac{\Delta\Pi_{\perp}}{\Delta A} \quad (2)$$

where ε^* is the complex dilatational modulus, G^* is the complex shear modulus and $\Delta\Pi_{\parallel}$ and $\Delta\Pi_{\perp}$ are the lateral pressure fluctuation registered by the plates placed parallel or perpendicular to the barriers displacement axis, respectively.

The loss and storage component of each complex modulus can be computed knowing the retardation angle (φ). If the layer is purely elastic, then area and Π should always be in phase; if it is purely viscous, both parameters should be 90° out of phase. The frequency dependent dilatational complex modulus $\varepsilon^*(\omega)$ is commonly defined as:

$$\varepsilon^*(\omega) = \varepsilon'(\omega) + i\varepsilon''(\omega) = \varepsilon'(\omega) + i\omega\eta_d(\omega) \quad (3)$$

where the real part $\varepsilon^*(\omega)$ corresponds to the dilatational elasticity, while the imaginary part $i\omega\eta_d(\omega)$ corresponds to the dilatational viscosity. The elastic (storage), ε' and viscous (dissipative) ε'', components of the dilatational modulus can be calculated from:

$$\varepsilon' = |\varepsilon| \cos\varphi \quad (4)$$

$$\varepsilon'' = |\varepsilon| \sin\varphi \quad (5)$$

In the same way, the frequency dependent shear complex modulus $G^*(\omega)$ defined as:

$$G^*(\omega) = G'(\omega) + iG''(\omega) = G'(\omega) + i\omega\eta_s(\omega) \quad (6)$$

The elastic G', and viscous G'', components of the shear modulus can be calculated from:

$$G' = |G| \cos\varphi \quad (7)$$

$$G'' = |G| \sin\varphi \quad (8)$$

being $\varphi = 2\pi\omega\delta t$ the phase shift angle calculated from the time lapse (δt) between A and Π signals at Π_0

In this work, only one pressure sensor was used and the position of the Whilhelmy plate was oriented parallel and perpendicular consecutively during the same experiments. Changing the order of the determinations (first parallel or perpendicular) did not alter the obtained results.

2.5. Measurements of interfacial diffusion coefficient of beads

Micro-beads were cleaned by successive centrifugation steps followed by removing the supernatant; the pellet (beads) was suspended in MQ water. This procedure was repeated 10 times. Just before use, this bead suspension was sonicated, in order to avoid bead aggregation, and a low amount of this solution was added to the DMSO peptide solution (0.5%, v/v). The resultant suspension was used as the spreading solution to form the monolayer. This low amount of beads neither affect the mean molecular area nor the collapse pressure and the general surface behaviour of peptide monolayers.

The calculation of D_{exp}, the diffusion coefficient of the beads, was performed as previously described [31,33]. Briefly, videos of the monolayer were recorded for 6–9 s at 33 frames s^{-1}. The original gray-scale images were converted to binary (black/white) images using Image J software. For this, the slightly non-uniform illumination in the images was discarded using a band-pass filter and then, a particular gray-scale level (threshold) was selected, and all pixels with intensities above this value were converted to "white" while the pixels with intensities below this threshold level were converted to "black". The value of the threshold level was determined on the basis of an optimal resolution of the structures by constant comparison with the original picture. The trajectories of the beads were followed through the 200–300 frames using the plug-in "Mosaic" of Image J software [34]. Since convection may be diminished but not completely cancelled, D_{exp} was calculated from the trajectories of two beads that suffer similar convection drag (it was considered that at close enough distance, $\leq$30 μm, beads suffered the same drag). However, beads that were too close to each other (less than 10 μm) were not selected, since capillarity effects between each particle could be influencing their motion. It was assumed that all the analysed beads were at the interface and not in the subphase, since *i)* no beads were found at higher focuses and *ii)* the tracked beads were in the focus during all of the recording (their motion was only two-dimensional).

Considering the relative position of beads ($\vec{X}$) at different time lapses between frames (δt), the Mean Square Displacement can be calculated as $MSD = |\vec{X}^{t+\delta t} - \vec{X}^{t}|^2$ MSD was plotted as a function of δt for each pair of beads and, since beads were of the same size (beads aggregates were not chosen for the analysis), the diffusion coefficient is expected to be approximately the same. At these conditions, $MSD = 8D\delta t$ ⟨REFNUMLINK⟩[31,35].

Monolayer shear properties affect beads lateral diffusion in a complex manner that depends on the degree of sinking and the wetting of the beads [36]. Since these factors where unknown, we directly compared the D values at each condition without determining the shear moduli. As a film becomes more responsive upon shear strain, the bead diffusion becomes precluded and therefore, D is expected to decrease, correlating with films with a higher shear stress.

2.6. Secondary structure determinations of Melittin: FT-IR and ATR

FT-IR spectra of Mel (6 mg/ml) in 15% SDS (^2H_2O) were acquired on a Nicolet Nexus spectrometer (continuously purged with dry air to eliminate water vapor interference) at room temperature in a CaF_2 cell with a 0.1 μm Teflon spacer. 100 scans were signal-averaged at a resolution of 2 cm^{-1}. Spectra of peptide-free samples were subtracted from the spectra of Mel containing samples, using the OMNIC E.S.P. 5.1 software. Fourier self-deconvolution was performed using a bandwidth of 18 cm^{-1} and an enhancement factor of 2. Alkaline solutions were prepared by titration with NaOD (Sigma Chem. Co., USA).

ATR-FTIR spectra of Mel (1 μg μL^{-1} in H_2O with and without 50 mM NaOH) were recorded on an Equinox 55 IR spectrophotometer (Bruker Optics) equipped with a single reflection diamond reflectance accessory (Golden Gate, Specac). The spectrometer was continuously purged with dried air. A total of 256 accumulations were performed to improve the signal/noise ratio. Spectra were recorded at 21 °C using a resolution of 2 cm^{-1}. The peptide sample (1.5–5 μL) was spread on the diamond crystal surface and the excess solvent (water) was removed under nitrogen flow. For the secondary structure analysis the water vapor and side chain contributions were subtracted and then the spectra were baseline corrected and normalized for equal area between 1700 and 1500 cm^{-1}. All spectra were deconvoluted using a Lorentzian deconvolution factor with a full width at the half maximum of 20 cm^{-1} and a Gaussian apodization factor K = 1.5. The bands identified in the deconvoluted spectra were used for curve fitting of the deuterated original (K = 1) spectra using Gaussian/Lorentzian bands [37].

3. Results

3.1. Compression isotherms of pure peptide monolayers

Fig. 1a shows lateral compression isotherms (expressed as a function of surface density) of Mel monolayers. As previously reported [15], films of this peptide are stable up to a collapse pressure (Π_c) of 15 mN m^{-1} at pH 5.6 and become more stable when an alkaline subphase is used (Π_c = 24 mN m^{-1} at pH 11, see Figs. S1 and S2). Associated with this increase in lateral stabilization in almost 10 mN m^{-1}, the surface potential (ΔV) diminished more than 100 mV, see Figs. S1 and S2. Both, lateral stability (Π_c) and surface potential at maximum packing (ΔV_c) present a pronounced variation between pH 9 and 11, very probably related with the ionization of the lysines, the only titratable residues in this pH range. Mel formed stable monolayers at both pHs and did not exhibit hysteresis when compression/expansion cycles were performed from 1 mN m^{-1} up to collapse pressure (see Fig. S2).

Aβ1-42 peptide isotherms were also in agreement with those previously published [18,19]. Both Aβ1-40 and Aβ1-42 exhibit indistinguishable compression isotherms, developing stable peptide monolayers of high stability against lateral compression and reaching lateral pressures as high as ~30 mN m^{-1} (Fig. 1a). β-amyloid peptide films were less densely packed than Mel films and, contrary to the latter, showed a marked hysteresis upon compression-expansion cycles (Fig. S3).

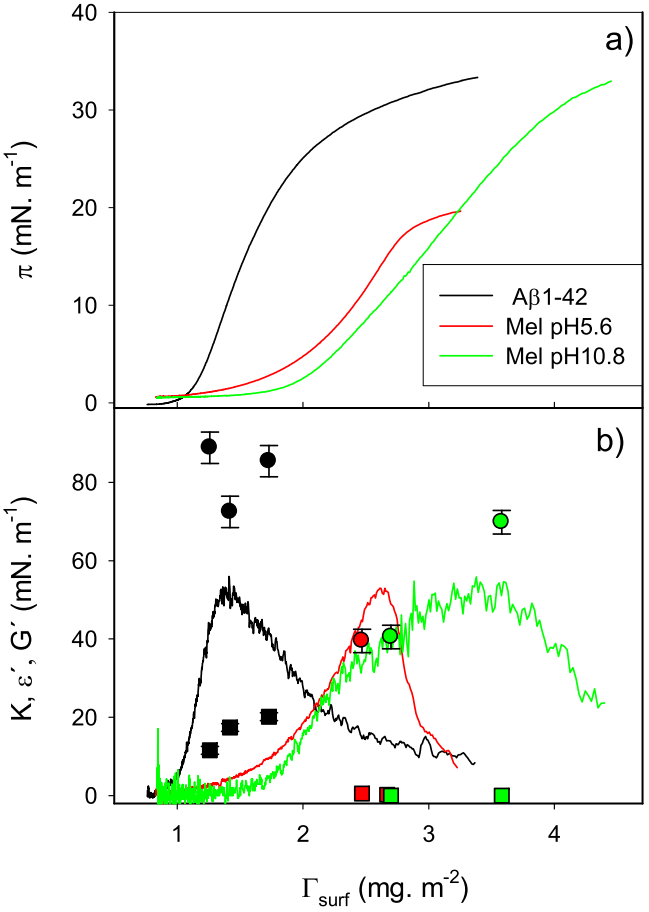

Fig. 1. Surface properties of peptide monolayers at the air/water interface. (a) Monolayer compression isotherms of peptides expressed as a function of surface mass density (Γ_{surf}). (b) Compressibility moduli K (lines), elastic dilatational ε'(circles) and elastic shear G'(squares) moduli. See colour code in legend for the different peptide monolayers.

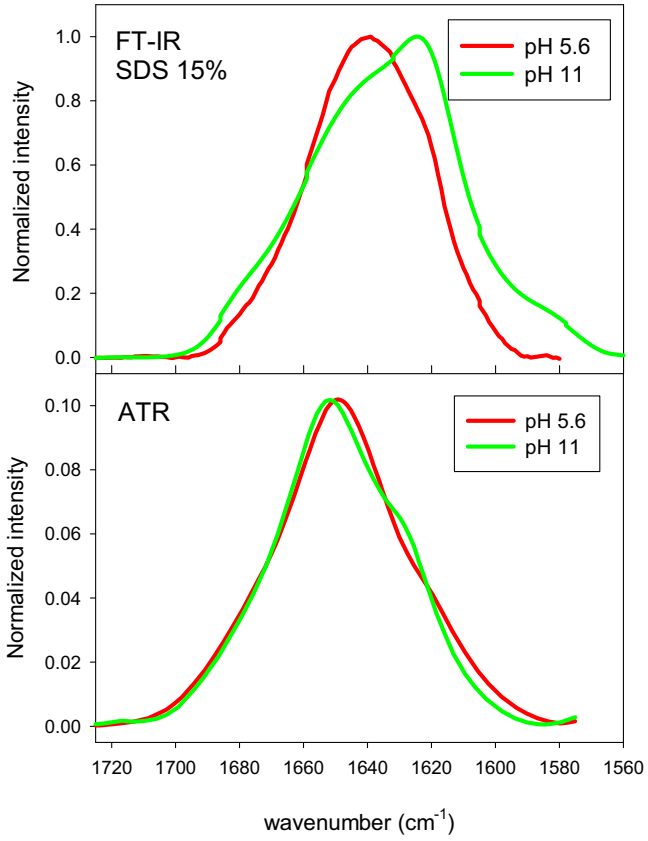

Fig. 2. Effect of pH on secondary structure of Melittin. (a) FT-IR of Mel in the presence of SDS micelles (SDS 15%). (b) ATR of Mel deposited onto a diamond surface. Red line: pH 5.6. Green line: pH 11 (alkaline). (For interpretation of the references to colour in this figure legend, the reader is referred to the web version of this article.)

The compressibility modulus parameter K, which relates the variation of the lateral pressure with the mean molecular area (MMA), is given by:

$$K = MMA\left(\frac{\partial \Pi}{\partial MMA}\right)_T \quad (9)$$

and it has been reported to correlate with the secondary structure of peptides [11]. This parameter is inversely related to compressibility of monolayers and its maximum value is typically associated with two dimensional phase transitions for lipid films [38]. As it can be observed in Fig. 1b, the Kcurves of the different peptide monolayers were similar, reaching maximal values of ~50 mN m^{-1}. Contrary to previously observed [11] in the systems studied here the lateral stability (measured from the collapse pressure, Π_C) did not correlate with the compressibility modulus. Furthermore, these values are much lower than those observed for shorter peptides (13 residues) known to form crystalline β-sheet monolayers (115 < K <172 mN m^{-1}) and that are able to suffer out of plane backbone bending after reaching a certain critical molecular assembly [39], that it does not seem to be the case for naturally occurring amyloid peptides. However, it should be mentioned that the compressibility modulus an overall parameter, and that, when determined from an anisotropic compression isotherm, it may enclose completely different behaviours from each composing parameter, *i.e.*, the viscous and the elastic components of the dilatational (ε) and shear (G) contributions. These parameters are evaluated in detail below, and finally analysed together with the secondary structure and the monolayer topography obtained by BAM.

3.2. Secondary structure of Melittin at alkaline subphases

It was previously proposed that monolayers prepared with β-sheet peptides are more stable against lateral compression (*i.e.*, collapse at higher lateral pressures) and less compressible than α-helix peptides [11,12]. As shown in Fig. 1, Mel showed a more stable monolayer at higher pH (above pH 11) compared with pH 5.6. In order to assess whether there is a conformational change on the peptide secondary structure at pH 11, we performed FT-IR measurements of Mel at pH 5.6 and 11 in absence and in presence of SDS micelles, a membrane-mimetic system reported as an excellent promoter of α-helix for Mel at neutral pH [40]. In presence of SDS micelles at pH 5.6, a unique peak centred at 1640 cm^{-1} was observed, indicating a mixture of α-helix and random structure (Fig. 2a). At pH 11, a prevailing peak at 1624 cm^{-1} was observed, indicating an increase in β-sheet contribution. On the other hand, ATR measurements of pure Mel adsorbed to a diamond surface showed a unique 1650 cm^{-1} peak when dried from a solution at pH 5.6, indicating an α-helix as the main secondary structure, while a shoulder at 1628 cm^{-1} appears when the peptide was deposed onto the surface from a solution at pH=11 (Fig. 2b). This indicates that a β-sheet structure was adopted by Mel at high pH when the peptide was in solution and strengthens the idea that the higher stability and reduced surface potential of Mel monolayers observed at pH 11 in comparison to those values obtained at pH 5.6 may be due

to a peptide conformational change from mainly α-helix to other with an important content in β-sheet structure.

3.3. BAM images of peptide monolayers

In order to evaluate whether the morphology of peptide monolayers at the micron level differs for α-helical peptides compared to β-sheet peptides, we directly observed the peptide films at the air-water interface using Brewster Angle Microscopy (BAM). Fig. 3 shows BAM images of Mel monolayers, at pH 5.6 and 11, and those of Aβ1-42 films at pH 5.6. All of them were homogeneous from the lift-off area up to the maximal packing pressure (15 and 25 mN m^{-1} for Mel monolayers at pH 5.6 and 11, respectively and 30 mN m^{-1} for Aβ1-42 films). Interestingly, Aβ1-42 monolayers appeared to be heterogeneous before the lift-off area, with a typical topography of solid-like patches (brighter regions) immersed in a gaseous film (darker regions). This kind of topography was never observed in Mel monolayers at any surface density (even at very large mean molecular areas, about the double value of that observed at lift-off point) at both pH assayed. This behaviour observed for the amyloid peptides may be related with higher cohesive interactions in the Aβ1-42 films (similar results were obtained for Aβ1-40 peptide). The homogeneity observed in Mel (at both pHs) and Aβ1-42 monolayers (from lift-off area to collapse pressure) is in keeping with their compression isotherms in which they did not present any evidence of phase transition or discontinuity. These results are important because rheological properties of peptide films could be governed by the properties of one of the coexisting regions, if lateral heterogeneity were present. From our BAM experiments, this can be discarded.

3.4. Macroscopic rheological behaviour of pure peptide monolayers

So far, we have shown that although monolayers of both amyloid peptides, Aβ1-40 and Aβ1-42, were more stable against lateral compression than those formed by the α-helical peptide Mel [12,18] their compressibility moduli (an overall rheological parameter) exhibited similar values. In addition, all peptides showed homogeneous films at lateral packing with higher densities than at the lift-off area without the evidence of microdomains. From this, and in order to gain insight into peptide molecular lateral interactions, we performed experiments to determine the rheological properties of films formed by either α-helical or β-sheet peptides. Firstly, we measured the monolayer shear and dilatational properties by means of oscillatory anisotropic compression experiments of peptide monolayers. Mel monolayers spread on subphases at pH 5.6 yielded an elastic dilatational modulus (ε') of 40 ± 3 mN m^{-1} and a negligible elastic shear modulus (G′)(1 ± 1 mN m^{-1}) when oscillating around 15 mN m^{-1} at 10 mHz and 3% ΔA, whereas the dilatational and shear viscosity moduli were below the resolution of the technique. These four rheological parameters were unaffected when the pH of the subphase was increased to 11 ($\varepsilon\acute{\imath}$ = 41 ± 3 mN m^{-1} and negligible *Gí*at 15 mN m^{-1} at both pHs, see Table 1). Since Mel monolayers spread over subphases at pH 11 were stable up to higher pressures than at pH 5.6, oscillations were also performed at 25 mN m^{-1} where the measured *Gí* modulus was negligible but the $\varepsilon\acute{\imath}$ modulus increased to 72 mN m^{-1} (see Table 1).

Oscillation experiments performed with monolayers composed of the Aβ1-40 and the Aβ1-42 peptide led also to negligible viscosity moduli. Table 1 summarizes both, dilatational and shear elasticities at the same oscillation conditions (around 15 mN m^{-1} at 10 mHz and 3% ΔA). Amyloid peptides presented a different rheological behaviour compared to Mel, exhibiting higher elastic shear component and higher dilatational moduli. It should be mentioned that, since the behaviour of Aβ1-42 exhibited hysteresis, $\Delta\Pi_{\parallel}$ and $\Delta\Pi_{\perp}$ might have been overestimated, however their relation should be the same and thus the values obtained for *Gí* were a good approximation.

Table 1
Elastic contributions to the rheological behaviour of peptides monolayers at 15 mN.m^{-1}.

Peptide	ε' (mN.m^{-1})	G' (mN.m^{-1})
Mel pH 5.6 (α-helix)[a]	40 ± 3	<1
Mel pH 11 (partial β-sheet)	41 ± 3	<1
Mel pH 11[b] (partial β-sheet)	72 ± 3	1 ± 1
Aβ1-40 (mostly β-sheet)[c]	85 ± 5	19 ± 1
Aβ1-42	80 ± 4	19 ± 1

[a] Refs. [16,17].
[b] Measured at 25 mN m^{-1}.
[c] Refs. [19,20].

It should be highlighted that both, shear and dilatational viscous moduli were not detected with this technique, in contrast to many shear resistant proteins whose corresponding moduli present both elastic and viscous components [1,9].

Fig. 1b shows both $\varepsilon\acute{\imath}$ and *Gí* (symbols) together with the *K* modulus (continuous lines) at varying peptide surface concentrations (Γ_{surf}). For Aβ1-42, a Γ_{surf} variation from 1.3 to 1.8 mg m^{-2} (*i.e.*, Π from 5 to 20 mN m^{-1}) correlated with a *Gí* increment from 11 to 19 mN m^{-1}. At these densities, *K* exhibited values around 50 mN m^{-1} whereas $\varepsilon\acute{\imath}$ values were between 75 and 90 mN m^{-1}. Thus, *K* exhibited intermediate values between $\varepsilon\acute{\imath}$ and *Gí*, which highlight the idea that the compressibility modulus alone is insufficient to characterize the rheological behaviour of peptides at the interface since it depends on both, shear and dilatation in a non-linear fashion as a consequence of the non-isotropic compression that is usually employed.

On the other hand, for Mel monolayers at pH 5.6, G' was negligible and ε' was equal to *K*, which is coherent with the idea that the dilatational moduli are enough to characterize its rheological behaviour, as in the case of most lipids. In contrast, Mel monolayers at pH 11 exhibited comparable values of $\varepsilon\acute{\imath}$and *K* at 15 mN m^{-1} but if further compression was performed, a divergence between these parameters was observed ($\varepsilon\acute{\imath}$ = 72 while *K* = 50 mN m^{-1}). In summary, with this technique we were able to distinguish differential rheological behaviours under a dilatational and a shear strain for monolayers of Mel and amyloid peptides. However, although $\varepsilon\acute{\imath}$ differs from *K* in Mel at pH 11 and at high lateral pressures, we did not find a marked difference of the Mel behavior at different pHs. As this could probably be due to the resolution of the oscillatory technique, we also performed experiments using a micro-rheological approach based on bead diffusion measurements on monolayers.

3.5. Micro-rheology of peptide monolayers

The micro-rheological approach is useful to obtain information of rheological properties of materials that present low stress response upon a shear strain [36]. Following this approach, a quantitative comparison of the shear modulus of different monolayers can be achieved by tracing the Brownian motion of beads at the interfaces and calculating their interfacial diffusion coefficient (*D*). From the obtained values we were able to evaluate quantitatively whether there was an effect of pH in the rheological properties of Mel, which were below the resolution of the oscillatory technique and, in addition, we compared such behaviour with amyloid peptide monolayers.

Fig. 4b shows the *D* values of beads diffusing on monolayers of Mel, at both pH 5.6 and 11, and of Aβ1-40 at different surface pressures. The data clearly show that Mel exhibited π-dependent *D* values; at low lateral packing (2 mN m^{-1}) *D* values were high and comparable to those observed for beads at a clean saline/air

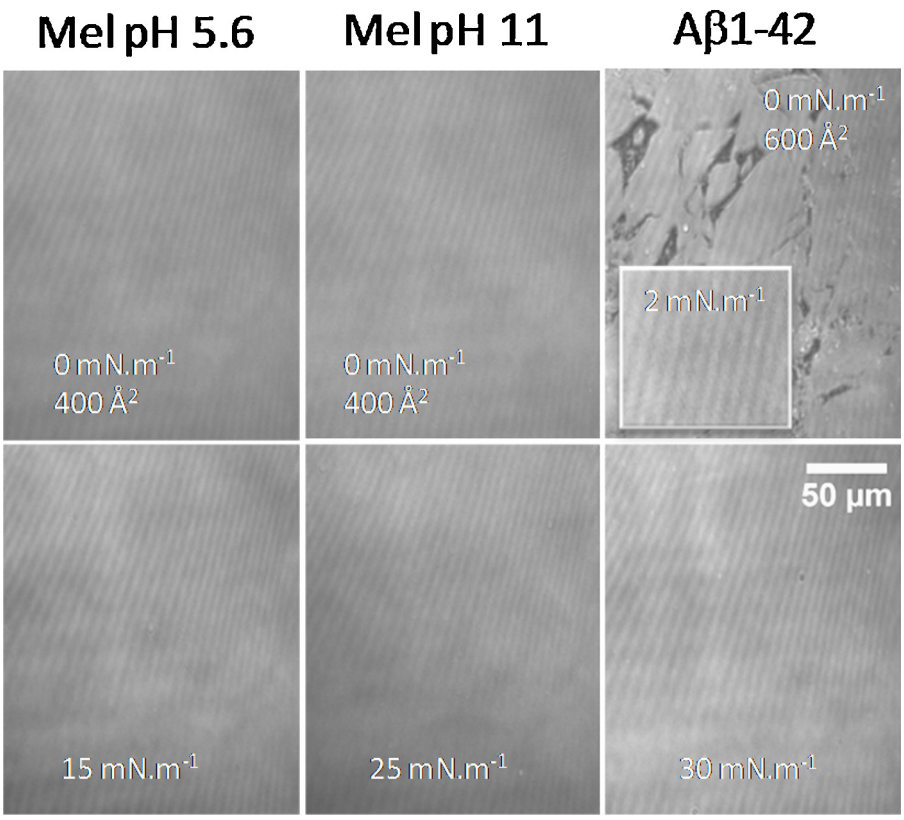

Fig. 3. Topography of pure peptide monolayers.
BAM micrographies of Mel at pH 5.6 (left panel), Mel at pH 11 (middle panel) and Aβ1-42 (right panel) monolayers immediately before lift-off and at collapse pressure. The surface densities before lift-off area (0 mN m^{-1}) were 0.75, 1.5 and 0.5 mg m^{-2} for Mel pH=5.6 and pH=11 and Aβ1-42, respectively. Insert: Aβ1-42 show that at 2 mN m^{-1} the monolayers appear homogeneous.

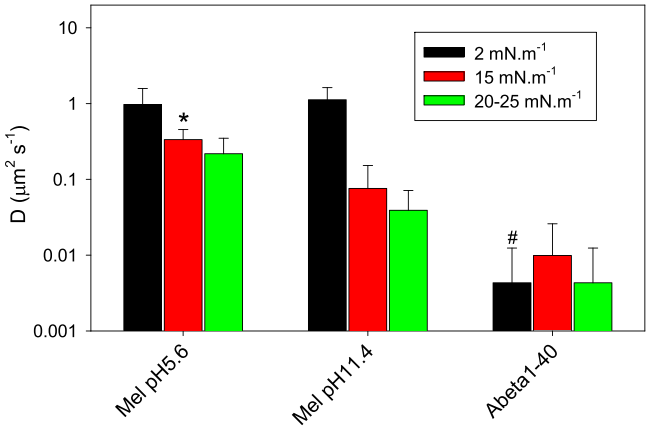

Fig. 4. Diffusion coefficient of beads (D) in pure peptide monolayers.
Statistically significant differences correspond to Tukey test between the three monolayers at each of the following lateral pressures: *= 15 mN m^{-1} (t-test: $p < 0.05$); # = 2 mN m^{-1} ($p < 0.001$). Note the log scale in y-axis (D).

interface (see Fig. 5 in Wilke et al. [31]). At higher surface pressures, D values were lower and with a marked dependence on pH, being smaller at pH 11 (lower than 0.2 µm^2 s^{-1}) compared to pH 5.6 (higher than 0.2 µm^2 s^{-1}). Contrary to Mel, monolayers of amyloid peptides always exhibited very low D values (around zero) even at 2 mN m^{-1}. It is worth to note that the D data range for Mel at high surface pressures was within the order of those found for liquid-expanded lipid monolayers (0.1 µm^2 s^{-1} < D < 0.3 µm^2 s^{-1}) and the D values measured for Aβ1-40 were comparable to liquid condensed lipid monolayers (D < 0.01 µm^2 s^{-1}) [31].

4. Discussion

4.1. Rheological differences between the β-sheet and α-helix peptides

The shear behaviour observed in many proteins has been attributed to the formation of a continuous gel-like network [41,42]. Firstly, it should be mentioned that although in some cases it has been attributed to the formation of intermolecular disulphide bridges (the reader can refer to Wierenga *et al.* [8] which reviews evidences in favour and against strong disulphide cross-linking), in our case, no disulphide bonds can be formed between the selected peptides molecules since they lack cysteine residues. Other authors suggested that interdomain interactions may affect the rheological properties of the film [43]. In this sense, BAM images show that amyloid peptide monolayers were homogeneous at surface densities higher than the lift-off area and their compressibility (K) curves suggest that no phase transitions occurred at π < 15 mN m^{-1}, suggesting that inter-domain interactions would not account for the shear stress observed for these amyloid peptides. On the other hand, the existence of condensed domains at the nanoscale (not detected by BAM) should be checked, as a domain (fibrillar) structure has been observed for shorter (12–13 residues length) amyloidogenic-like peptides [44,45]. For amyloid peptides this may be the case, as BAM images suggest a gas-condensed phase coexistence at π = 0. In such a molecular (fibrillar) structure, large domain structure is the consequence of intermolecular hydrogen bonds [39,45] leading to condensed domains interacting sterically and assembling into large anisotropic zones/patches of the monolayer [44]. If the molecular arrangement of naturally occurring amyloids peptides at surfaces is similar to the domains described

Table 2
Parameters obtained from a scaling behaviour fitting of a K-Γ_{surf} and from the prediction of the onset of shear as a consequence of steric jamming.

Condition/peptide	y_{eq}	ν	Γ^*	Γ^{max}	Γ
Melittin pH 5.6	4.65	0.637	1	2.5	1.65
Melittin pH 11	7.2	0.581	1	2	1.22
Aβ1-42	9.3	0.56	0.75	1.4	0.84
β-lactoglobulin[a]	5.5	0.61	0.37	0.75	0.73

[a] Taken from Ref. [9].

to other shorter amyloidogenic-like peptides mentioned above, a marked shear response would be expected.

In the absence of intermolecular interactions leading to large domain/zones/patches formation, it is still possible to expect a shear response. According to an alternative model, the shear elasticity results from the low mobility of the densely packed proteins [8]. By analysing β-lactoglobulin monolayers, Cicuta and Terentjev [9] have proposed steric jamming (dynamical arrest by hard-core repulsive interactions) as a common feature determining the onset of shear for polymer (protein) monolayers.

Then, both hydrogen bonding and/or repulsive (electrostatic or steric hindrances leading to dynamical arrest) could be responsible for the marked shear modulus observed in amyloid peptides. Considering the pKa of the constituting aminoacids of these peptides, a network of repulsive electrostatic interactions is not likely to explain the observed differences: the monolayers of β-amyloid peptides are neutral at pH 5.6 whereas Mel bears a +5 net charge at pH 5.6 and ≅+1 at pH 11. The steric jamming alternative is considered below.

4.2. Scaling behaviour of peptide monolayer isotherms

It has previously been published that the isotherms of many proteins at interfaces can be statistically described by the Flory theory applied for polymer monolayers in the "semi-dilute" regime (*i.e.*, between the lift-off area and 2–7 mN m^{-1}). This description stays that monolayersí surface pressure and compressibility vary as a function of mass density following a power law ($K = c\Gamma_{surf}^{y_{eq}}$). This "scaling behaviour" was evaluated for our peptides. It can be observed that the three monolayers could be well fitted to this model in a wide range of surface pressures (see Figs. S4 and S5 in Supplementary data). By comparison, the isotherm of a lipid forming liquid expanded monolayers was added in order to show an isotherm that doesnít fit to this model (a scaling behaviour was observed only up to very low surface pressures, see Fig. S6). It should be noted that, as mentioned above and suggested by others [44], in the case of amyloid peptides, a nanoscale domain formation should not be discarded. In such a case, application of the Flory theory would be inappropriate, in spite of the good fit of the data, and alerts over other systems that have been analysed in this way.

The scaling exponent is related to the Flory exponent (ν) through $y_{eq} = 2\nu/(2\nu - 1)$ According to Vilanove and Rondelez [46], the monolayers studied here are in semi-dilute regime with Flory exponent between good solvent ($\nu = 0.75$) and theta-solvent ($\nu = 0.57$) conditions. These conditions mean that monomers inside a chain behave as a self-avoiding random walk ($\nu = 0.75$) whereas the expansive effect of intramolecular monomer exclusion is counterbalanced by a preferential attraction between them in the theta-solvent condition ($\nu = 0.57$). In this way, Aβ1-42, presenting $\nu = 0.56$, would be indicating less peptide solvation at the interface than β-lactoglobulin ($\nu = 0.61$, taken from Ref. [9]) and Mel ($\nu = 0.64$ and 0.58 at pH 5.6 and 11, respectively), Table 2. This is in keeping with stronger intramolecular interactions for amyloid peptides (in agreement with the observed segregation of a condensed/solid like phase of these peptides in the BAM images at high mean molecular areas) at very low surface density (See Fig. 3).

On the other hand, we followed the analysis described by Cicuta and Terentjev [9]. for β-lactoglobulin, where the density at the onset of shear (Γ) was predicted considering it as a consequence of steric hindrance of the molecules that have been so compressed that can be assumed as jammed rigid disks. In this approach, it is assumed that a shear strain σ induces a deformation that is equivalent to a local additional compression. The equation that express the energy cost (ΔF) of compressing chains to be consider as hard disks (when $\Delta F \geq k_B T$ each chain molecule can be considered a hard disk and hence the shear emergence); (see Eq. (17) of Ref. [9]) is:

$$\Delta F = k_B T \left[\left(\frac{1}{1-\sigma} \right)^{y_{eq}-1} - 1 \right] \left(\frac{\Gamma}{\Gamma^*} \right)^{y_{eq}-1} \quad (9)$$

Then, the density at the onset of shear (Γ) can be calculated knowing: *i)* the fitting parametery_{eq}, related to the Flory exponent through $y_{eq} = 2\nu/(2\nu - 1)$, *ii)*Γ^*, the surface density at the isotherm lift-off area and *iii)*σ, the strain used to oscillate the barriers;

According to this analysis, Mel monolayers at both pHs (reaching densities equal to Γ^{max} = maximum density up to which the best fitting curve holds) clearly exceeded the predicted surface density necessary for the onset of a shear behaviour (Γ, Table 2) and, however, this behaviour was not observed. This suggests that steric hindrances are not enough to generate a shear response in these peptide monolayers. The micro-rheological differences sensed in Mel when the pH was changed (Fig. 4) would correlate with the increase in β structure. Furthermore, the marked difference in the shear modulus in amyloid peptides (mainly β-sheet structured) compared to Mel at neutral pH (mainly α-helix structured) suggest that the structure of the peptide modulates the shear properties of the film they are forming. A peptide with an extended β-sheet structure at the interface may impose intermolecular interactions along the whole film, thus it is not surprising that this kind of film forming peptides present a high inter-molecule cohesion and hence, with important shear moduli. This is in agreement with the high cohesive interactions observed for amyloid films at very low film densities as detected by BAM (Fig. 3).

5. Conclusions

β-amyloid peptides, which are known to present high percentages of β-sheet structure at the air water interface, exhibited interfacial rheological properties characterized by a marked response upon a shear strain. The latter property was found to be identical in monolayers composed of either Aβ1-40 or Aβ1-42. Both amyloid peptide monolayers presented a high micro-rheological shear stress even at low surface pressures and exhibited high shear elasticity, indicative of a solid network. Furthermore, this correlated with a theta-solvent condition, indicating poorer peptide solvation at the interface compared with Mel or with the published β-lactoglobulin [9].

In contrast, Mel monolayers exhibited a different rheological behaviour, which was dependent on pH. At comparable lateral pressures, the micro-rheological shear properties of Mel monolayers were higher at alkaline pH, which correlates with the high lateral stability found for Mel at alkaline pH. FT-IR measurements in bulk indicated a change in the secondary structure of Mel with an increase in bulk pH, towards a higher content in β-sheet structure, regardless being in pure form or associated to SDS micelles. Although Mel at high pH became more stable at air-water interface, this peptide did not exhibit a shear elasticity comparable to amyloid peptides. However, the diffusion of particles in this monolayer were intermediate between those found for α-helix Melittin (pH 5.6) and the β-sheet structured amyloid peptides. This is in line

with the percentage of beta-sheet structure, which increases in the order Mel (pH5.6) < Mel (pH11) < Aβ1-40/42.

In summary, even when Mel monolayers exceeded the surface concentration predicted for the onset of shear as a consequence of steric jamming, shear stress was still negligible in these films. Furthermore, a non-negligible shear modulus was determined for beta amyloid films, even though these monolayers were less densely packed than the α-helix Mel. Both results suggest that for small peptides, lateral interactions other than steric jamming are responsible for such behaviour. Clearly, the most evident interactions for these systems are the hydrogen bonds, which in the films formed by peptides with a β-sheet secondary structure determine an infinite lateral network.

Acknowledgements

This work was supported by grants from SECyT-UNC, FONCYT-MinCyT and CONICET, (Argentina). B.C. was working as postdoc associated to PICT-1784 (FONCYT, Argentina). E.A., N.W. and G.D.F are members of the Scientific Research Career (CIC) from CONICET (Argentina).

Appendix A. Supplementary data

Supplementary data associated with this article can be found, in the online version, at http://dx.doi.org/10.1016/j.colsurfb.2016.06.003.

References

[1] B.S. Murray, Rheological properties of protein films, Curr. Opin. Colloid Interface Sci. 16 (2011) 27–35.
[2] R. Mezzenga, P. Fischer, The self-assembly, aggregation and phase transitions of food protein systems in one, two and three dimensions, Rep. Prog. Phys. 76 (2013) 046601.
[3] M.A. Bos, T. van Vliet, Interfacial rheological properties of adsorbed protein layers and surfactants: a review, Adv. Colloid Interface Sci. 91 (2001) 437–471.
[4] I. Lopez-Montero, E.R. Catapano, G. Espinosa, L.R. Arriaga, D. Langevin, F. Monroy, Shear and compression rheology of Langmuir monolayers of natural ceramides: solid character and plasticity, Langmuir 29 (2013) 6634–6644.
[5] J. Kragel, S.R. Derkatch, R. Miller, Interfacial shear rheology of protein-surfactant layers, Adv. Colloid Interface Sci. 144 (2008) 38–53.
[6] R. Miller, J.K. Ferri, A. Javadi, J. Kragel, N. Mucic, R. Wustneck, Rheology of interfacial layers, Colloid Polym. Sci. 288 (2010) 937–950.
[7] J. Pelipenko, J. Kristl, R. Rosic, S. Baumgartner, P. Kocbek, Interfacial rheology: an overview of measuring techniques and its role in dispersions and electrospinning, Acta Pharm. 62 (2012) 123–140.
[8] P.A. Wierenga, H. Kosters, M.R. Egmond, A.G. Voragen, H.H. de Jongh, Importance of physical vs. chemical interactions in surface shear rheology, Adv. Colloid Interface Sci. 119 (2006) 131–139.
[9] P. Cicuta, E.M. Terentjev, Viscoelasticity of a protein monolayer from anisotropic surface pressure measurements, Eur. Phys. J. E Soft Matter 16 (2005) 147–158.
[10] D. Langevin, Surface shear rheology of monolayers at the surface of water, Adv. Colloid Interface Sci. 207 (2014).
[11] R. Maget-Dana, D. Lelievre, A. Brack, Surface active properties of amphiphilic sequential isopeptides: comparison between alpha-helical and beta-sheet conformations, Biopolymers 49 (1999) 415–423.
[12] E.E. Ambroggio, G.D. Fidelio, Lipid-like behavior of signal sequence peptides at air-water interface, Biochim. Biophys. Acta 1828 (2013) 708–714.
[13] A. Renault, S. Pezennec, F. Gauthier, V. Vié, B. Desbat, Surface rheological properties of native and S-ovalbumin are correlated with the development of an intermolecular β-Sheet network at the air-Water interface, Langmuir 18 (2002) 6887–6895.
[14] S. Jordens, P.A. Ruhs, C. Sieber, L. Isa, P. Fischer, R. Mezzenga, Bridging the gap between the nanostructural organization and macroscopic interfacial rheology of amyloid fibrils at liquid interfaces, Langmuir 30 (2014) 10090–10097.
[15] G.D. Fidelio, B. Maggio, F.A. Cumar, Interaction of melittin with glycosphingolipids and phospholipids in mixed monolayers at different temperatures. Effect of the lipid physical state, Biochim. Biophys. Acta 862 (1986) 49–56.
[16] D. Blaudez, J.-M. Turlet, J. Dufourcq, D. Bard, T. Buffeteau, B. Desbat, Investigations at the air/water interface using polarization modulation IR spectroscopy, J. Chem. Soc. Faraday Trans. 92 (1996) 525–530.
[17] I. Cornut, B. Desbat, J.M. Turlet, J. Dufourcq, In situ study by polarization modulated Fourier transform infrared spectroscopy of the structure and orientation of lipids and amphipathic peptides at the air-water interface, Biophys. J. 70 (1996) 305–312.
[18] E.E. Ambroggio, D.H. Kim, F. Separovic, C.J. Barrow, K.J. Barnham, L.A. Bagatolli, G.D. Fidelio, Surface behavior and lipid interaction of Alzheimer beta-amyloid peptide 1–42: a membrane-disrupting peptide, Biophys. J. 88 (2005) 2706–2713.
[19] C. Schladitz, E.P. Vieira, H. Hermel, H. Mohwald, Amyloid β-sheet formation at the air-water interface, Biophys. J. 77 (1999) 3305–3310.
[20] G. Thakur, M. Micic, R.M. Leblanc, Surface chemistry of Alzheimer's disease: a Langmuir monolayer approach, Colloids Surf. B Biointerfaces 74 (2009) 436–456.
[21] C.E. Dempsey, The actions of melittin on membranes, Biochim. Biophys. Acta 1031 (1990) 143–161.
[22] M.A. Mendez, Z. Nazemi, I. Uyanik, Y. Lu, H.H. Girault, Melittin adsorption and lipid monolayer disruption at liquid–liquid interfaces, Langmuir 27 (2011) 13918–13924.
[23] H. Raghuraman, A. Chattopadhyay, Melittin: a membrane-active peptide with diverse functions, Biosci. Rep. 27 (2007) 189–223.
[24] M.L. Longo, A.J. Waring, L.M. Gordon, D.A. Hammer, Area expansion and permeation of phospholipid membrane bilayers by influenza fusion peptides and melittin, Langmuir 14 (1998) 2385–2395.
[25] M.T. Lee, T.L. Sun, W.C. Hung, H.W. Huang, Process of inducing pores in membranes by melittin, Proc. Natl. Acad. Sci. U. S. A. 110 (1424) 3–14248.
[26] K. Sasahara, K. Morigaki, K. Shinya, Effects of membrane interaction and aggregation of amyloid beta-peptide on lipid mobility and membrane domain structure, Phys. Chem. Chem. Phys. 15 (2013) 8929–8939.
[27] G.P. Eckert, W.G. Wood, W.E. Muller, Lipid membranes and beta-amyloid: a harmful connection, Curr. Protein Pept. Sci. 11 (2010) 319–325.
[28] T.L. Williams, L.C. Serpell, Membrane and surface interactions of Alzheimer's Abeta peptide–insights into the mechanism of cytotoxicity, FEBS J. 278 (2011) 3905–3917.
[29] C. Mollay, G. Kreil, H. Berger, Action of phospholipases on the cytoplasmic membrane of Escherichia coli. Stimulation by melittin, Biochim. Biophys. Acta 426 (1976) 317–324.
[30] N. Wilke, Chapter two – lipid monolayers at the Airâ€Water interface: a tool for understanding electrostatic interactions and rheology in biomembranes, in: I. Aleš, C.V. Kulkarni (Eds.), Advances in Planar Lipid Bilayers and Liposomes, Academic Press, 2014, pp. 51–81.
[31] N. Wilke, F. Vega Mercado, B. Maggio, Rheological properties of a two phase lipid monolayer at the air/water interface: effect of the composition of the mixture, Langmuir 26 (2010) 11050–11059.
[32] J.T. Petkov, T.D. Gurkov, B.E. Campbell, R.P. Borwankar, Dilatational and shear elasticity of gel-like protein layers on air/water interface, Langmuir 16 (2000) 3703–3711.
[33] B. Caruso, M. Villarreal, L. Reinaudi, N. Wilke, Inter-domain interactions in charged lipid monolayers, J. Phys. Chem. B 118 (2014) 519–529.
[34] I.F. Sbalzarini, P. Koumoutsakos, Feature point tracking and trajectory analysis for video imaging in cell biology, J. Struct. Biol. 151 (2005) 182–195.
[35] N. Wilke, B. Maggio, The influence of domain crowding on the lateral diffusion of ceramide-enriched domains in a sphingomyelin monolayer, J. Phys. Chem. B 113 (2009) 12844–12851.
[36] P. Cicuta, A.M. Donald, Microrheology: a review of the method and applications, Soft Matter 3 (2007) 1449–1455.
[37] H.J. Hilderson, G.B. Ralston, E. Goormaghtigh, V. Cabiaux, J.M. Ruysschaert, Determination of soluble and membrane protein structure by Fourier Transform Infrared Spectroscopy, in: Physicochemical Methods in the Study of Biomembranes, Springer, US, 1994, pp. 329–362.
[38] G.L. Gaines Jr, Insoluble Monolayers at Liquid-gas Interfaces, John Wiley & Sons, Inc., New York, 1966.
[39] V. Vaiser, H. Rapaport, Compressibility and elasticity of amphiphilic and acidic beta-sheet peptides at the air-water interface, J. Phys. Chem. B 115 (2011) 50–56.
[40] H. Raghuraman, A. Chattopadhyay, Effect of micellar charge on the conformation and dynamics of melittin, Eur. Biophys. J. 33 (2004) 611–622.
[41] A.H. Martin, K. Grolle, M.A. Bos, M.A.C. Stuart, T. van Vliet, Network forming properties of various proteins adsorbed at the Air/Water interface in relation to foam stability, J. Colloid Interface Sci. 254 (2002) 175–183.
[42] C.M. Wijmans, E. Dickinson, Simulation of interfacial shear and dilatational rheology of an adsorbed protein monolayer modeled as a network of spherical particles, Langmuir 14 (1998) 7278–7286.
[43] R. Krishnaswamy, V. Rathee, A.K. Sood, Aggregation of a peptide antibiotic alamethicin at the air-water interface and its influence on the viscoelasticity of phospholipid monolayers, Langmuir 24 (2008) 11770–11777.
[44] M. Lepere, C. Chevallard, G. Brezesinski, M. Goldmann, P. Guenoun, Crystalline amyloid structures at interfaces, Angew. Chem. Int. Ed. Engl. 48 (2009) 5005–5009.
[45] H. Isenberg, K. Kjaer, H. Rapaport, Elasticity of crystalline beta-sheet monolayers, J. Am. Chem. Soc. 128 (2006) 12468–12472.
[46] R. Vilanove, F. Rondelez, Scaling description of two-dimensional chain conformations in polymer monolayers, Phys. Rev. Lett. 45 (1980) 1502–1505.